REALIZATION OF DC- BUS SENSOR-LESS MPPT TECHNIQUE FOR A SINGLE-STAGE PV GRID-CONNECTED INVERTER

M.A. ELSAHARTY
Arab Academy for Science and Technology, Alexandria, Egypt
saharty@aast.edu

H.A. ASHOUR
Arab Academy for Science and Technology, Alexandria, Egypt
hashour@aast.edu

ABSTRACT

A single-stage photovoltaic (PV) grid connected system is an attractive approach for a distributed energy source due to its simple topology and low cost. However, maximum power point tracking (MPPT) algorithms require measurements on the DC side of the inverter in order to determine the operating point of the PV panel at each instant. This paper presents a sensor-less MPPT algorithm for a single-stage PV grid connected inverter where the MPPT algorithm determines whether the reference inverter operating point is below or beyond the maximum power point (MPP) at different light intensities based upon the current controller action. The proposed algorithm monitors the controller action after each perturbation, if the reference power is beyond the maximum power, the controller would saturate and thus the MPP is at the previous reference power. Changes in insolation are accompanied by changes in the current controller action, which is detected by the algorithm. The overall system has been experimentally implemented and control algorithm has been validated using digital signal processing (DSP) unit. Using simulation and practical implementation results, the performance of the proposed MPPT algorithm is evaluated while limits and merits of the proposed set have been demonstrated.

INTRODUCTION

The use of PV technology as a stand-alone energy source for grid-connected applications is an attractive approach due to its advantages of being adequately maintenance free and pollution free. The *MPPT* control technique plays an important role in this application since the system is required to extract maximum available power from the PV panel. Several topologies for grid-connected PV systems have been discussed in literature [1] involving single stage (DC/AC) and two stage (DC/DC/AC) converters. A challenging design target is to minimize the number of power electronic devices used by minimizing the number of power converting stages while maintaining a minimum number of sensing devices to ensure a low cost and less complex system.

Typical sensor-less *MPPT* algorithms discussed in [2-4], involve two stage converters with *MPPT* controller implemented on the DC/DC converter side by measuring only the DC bus voltage or converter output current while the DC/AC converter controller measures the inverter output current and grid side voltage for the current controller. Single stage converters discussed in [5] involve *MPPT* control algorithms based on DC bus voltage and PV panel current measurements while grid voltage and current are measured for current controller. In [6], PV panel voltage, grid current and grid voltage are measured for a single stage grid connected converter operating in continuous conduction mode for the configuration. It should be noticed that these *MPPT* algorithms require at least one sensing element on the DC side of the converter. Measurements on the DC side of the converter require filtering in order to determine the average DC component of the measured variable which eventually requires more processing.

In this paper, a current controlled, single-stage, single phase grid connected H-bridge inverter topology is utilized. A sensor-less *MPPT* algorithm is proposed and implemented based on perturbing the inverter reference output power and observing the inverter current controller action in order to achieve *MPP* operation.

DERIVATION OF THE PROPOSED TECHNIQUE

A. Single Stage Configuration Response

The proposed setup shown in Fig.1 consists of a typical single-stage PV grid connected inverter controlled via sinusoidal pulse width modulation (SPWM) technique. The P_{ref} is the reference output power, m_a is the amplitude modulation ratio of the *SPWM*, SW_1 and SW_2 are the inverter switches signal. Electrical signals: V_g and I_g as the grid voltage and current respectively, V_{dc} and I_{dc} are the PV panel voltage and current respectively, V_i is the inverter output voltage. Passive circuit components C_{dc}, R_1, L_1 are the dc link capacitor, filter inductor resistance and inductance respectively. Fig.2 depicts the typical simulated response of the proposed set for nine incremental values of P_{ref} , while Fig.3 illustrates the relation between PV panel and inverter characteristics for different operating regions. In Fig.4, at operating point 1 and 1', V_{dc} at that instant is less than the open circuit voltage of the PV panel and m_a is increased to m_{a1}. It should be noticed that V_{dc} should always be greater than V_i since an inverter operates in buck mode.

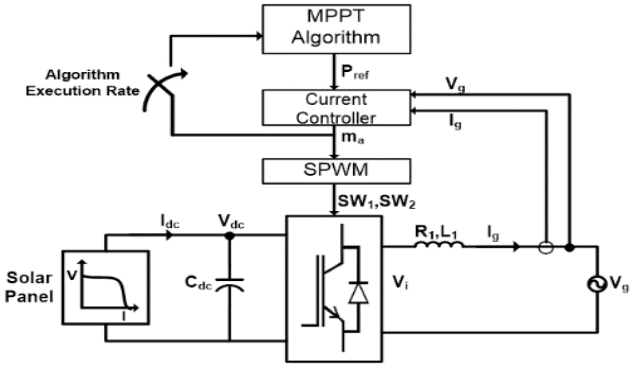

Fig.1. Proposed setup for sensor-less PV grid-connected MPPT system

Assuming sinusoidal I_g and V_g, the relationship between V_i and V_{dc} is given by (1) and (2).

$$V_i = m_a V_{dc} \quad \textbf{(1)}$$

$$|V_i| = \sqrt{\left(R_1|I_g| + |V_g|\right)^2 + \left(L_1\omega|I_g|\right)^2} \quad \textbf{(2)}$$

As P_{ref} is increases to operating point 2 and 2', V_{dc} further decreases while *Vi* increases thus according to Equation (1), m_{a1} would increase to m_{a2}. This can also be observed in Fig.2 in Region (3-4). In Fig.3, when the P_{ref} is equal to the *MPP* at operating point 3 and 3', m_{a3} indicates the maximum amplitude modulation ratio (m_{amax}) to operate the panel at the *MPP*. If P_{ref} is beyond *MPP*, V_{dc} would collapse as shown in Fig.2 in Region(6-9) and Fig.3. At this point, to achieve P_{ref}, a greater V_i is required which the PV panel is incapable of supplying. Thus it can be seen in Fig.2 that m_a increases beyond the linear region and saturates at the maximum value of linearity set by the controller. If a SPWM technique is used, m_{amax} for linear operation would be 1.

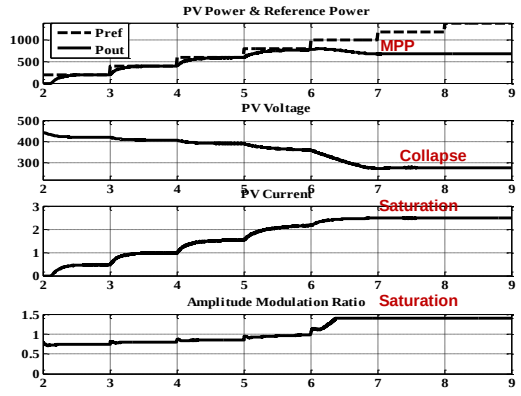

Fig.2. Typical response of the proposed system with incremental P_{ref}

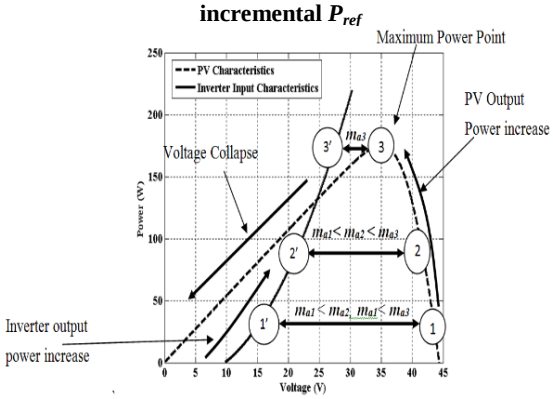

Fig.3. Inverter with filter and PV panel characteristics at different operating points

B. Effect of Change in Insolation

Changes in insolation would directly affect V_{dc} as shown in Fig.4. For a step increase in insolation in Region B→A, V_{dc} is increased and the controller would reduce m_a in order to maintain the same V_i, for the set P_{ref} as shown in Fig.5 (a). Whereas when insolation decreases there are two possible operation cases shown in Fig.4. If the current operating point (A) is less than the *MPP* at the lower insolation (B'), then m_a is expected to increase since the available V_{dc} has decreased as shown in Fig.5(b). Whereas if the current operating point (C) is greater than the *MPP* at the lower insolation (B'), the controller would eventually saturate, since V_{dc} is collapsing as shown in Fig.5(c).

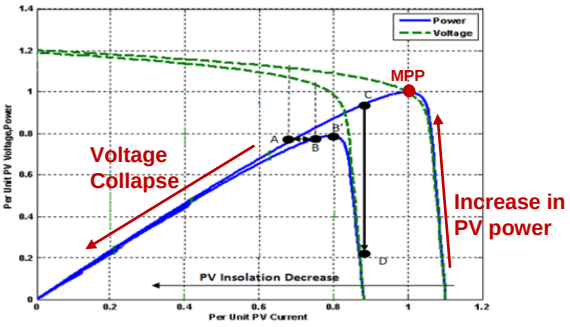

Fig.4. Effect of change in insolation on PV characteristics

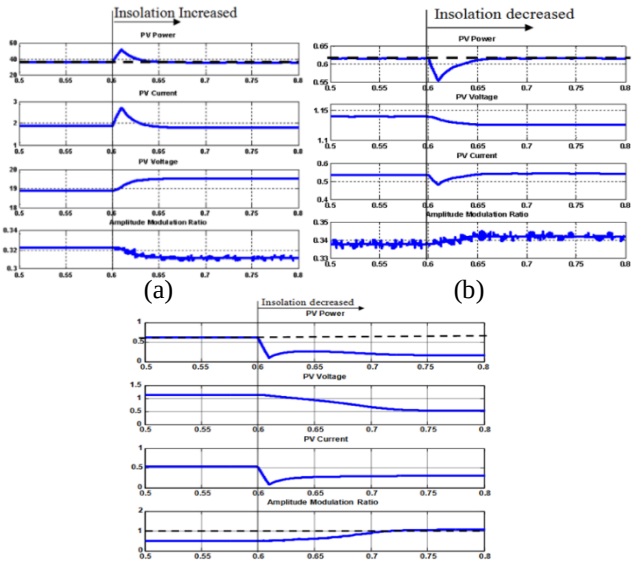

Fig.5. Change in P_{dc} , V_{dc} , I_{dc} and m_a (from top to down) referring to cases in Fig.4 for change in insolation (a) Point B to A (b) Point A to B and (c) Point C to D

It can be concluded from the previous analysis that m_a can be taken as an indicator for the PV operating region. This observation is utilized in the development of the proposed *MPPT* technique.

PROPOSED CONTROL ALGORITHM

A. Configuration

In the proposed setup shown in Fig.1, P_{ref} is perturbed based on the feedback information of m_a. The response of m_a is analyzed based on the *MPPT* algorithm and P_{ref} is then varied accordingly to always get the maximum available power from the PV panel.

B. Algorithm

The proposed *MPPT* algorithm given as a flowchart in fig.6 explains the method of decision making of increment/decrement to P_{ref}, based on the feedback m_a. The algorithm is based upon the following three processes:

Tracking process, as the P_{ref} is incremented, on regular basis, and m_a is observed. In the tracking process, the algorithm does not perform an increment to P_{ref} unless m_a is settled within a tolerance band. This is essential to avoid multiple increments during a slow transient state of the current controller yielding P_{ref} far beyond the MPP. In case m_a is settled and below m_{amax}, P_{ref} is stored as the maximum power (P_{MPPT}) and then P_{ref} is perturbed while m_a is observed in the next sampling interval. The process stops when m_a increases beyond the permissible m_{amax} which indicates a voltage collapse.

Recharging process, as the algorithm shifts to this process when P_{ref} is greater than the maximum available power point which is detected when m_a increases beyond m_{amax}. In order to move to the previous operating point, the DC link capacitor is required to be recharged since the current operating point voltage is below the *MPP* voltage. P_{ref} is reduced in order to recharge the DC link capacitor until m_a is below m_{amax}. At this state the *MPP* has been detected which is the last stored power increment (P_{MPPT}) before the voltage collapsed. When the DC link capacitor has been recharged, P_{ref} is set to P_{MPPT} and the algorithm shifts to the observation process while operating at the *MPP*.

Observation process, as in the final observation process the algorithm constantly checks m_a for changes which indicates a change in insolation. If m_a suddenly increases to m_{amax}, this would indicate a decrease in insolation and P_{ref} is beyond the *MPP*. The corrective action taken is to reduce P_{ref} to zero and starting the tracking process again. Whereas, when operating at the *MPP* and m_a decreases, this would indicate an increase in insolation which indicates that the *MPP* is beyond the current operating point. The corrective action would be to continue to the tracking process again.

C. Controller

The controller action is required to have a minimum overshoot in order to avoid m_a increasing beyond m_{amax} during the tracking process. The proposed controller shown in fig.7 illustrates the implemented controller structure. The integrator eliminates the error caused by the variable V_{dc} due to the non-linear V-I characteristics of the PV.

D. Parameters

The algorithm includes three parameters that are required to be adjusted; the *settlement range*, *algorithm sampling rate* and *reduction range*.

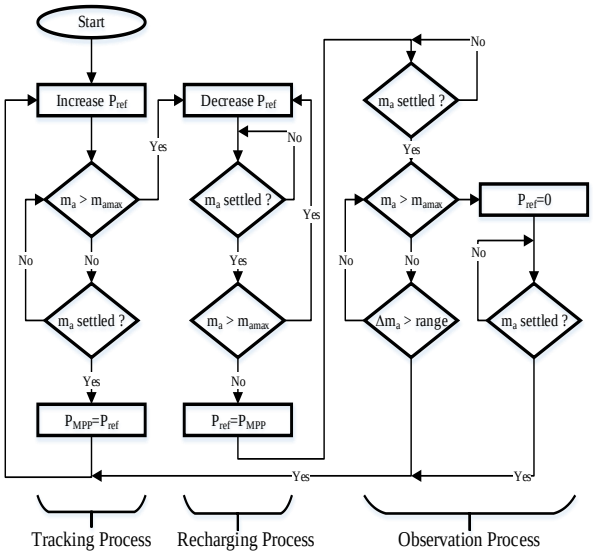

Fig.6 Flowchart of the proposed *MPPT* algorithm

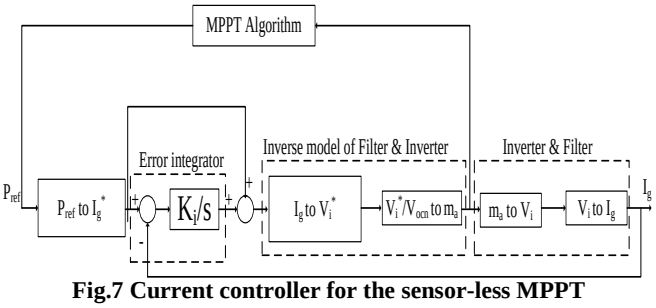

Fig.7 Current controller for the sensor-less MPPT

The *Algorithm Sampling Rate* is set so that it should be slower than the controller time constant (K_i), so that sufficient time is given to the controller to settle before the algorithm shifts to another state. Incase m_a is outside the *Settlement Range*, m_a would be considered as unsettled and the algorithm waits for m_a to settle to determine the next consecutive action. The algorithm would detect a reduction in m_a beyond the preset *Reduction Range*. At this state the algorithm waits for m_a to settle again within the *Settlement Range* to restart the tracking process. The *Settlement Range* should always be less than the *Reduction Range* in order to avoid misinterpreting oscillations to a m_a reduction.

To determine the *Reduction Range* due to insolation and/or temperature changes, the PV equivalent model is required. Equation (3) represents that model, where I_{pv} and I_o are the PV and saturation currents respectively, V_t is the thermal voltage, R_s and R_p are the equivalent circuit series and parallel resistance of the PV model. The corresponding values are given in Table I.

$$V = I_{pv} - I_o\left(e^{\frac{\left(V+\frac{R_S P}{V}\right)}{V_t}} - 1\right) - \frac{P}{V}\left(R_s + R_p\right) \quad \textbf{(3)}$$

E. Working Area

Fig.8 illustrates the inverter current controller action due

to an increase in insolation together with the associated variation of modulation index (m_a). The *MPPT* algorithm is required to detect the change in amplitude modulation ratio Δm_a in order to recognize that a new maximum power is available. A small change in insolation would lead to a decreased Δm_a and vice versa. Δm_a is described in (4) where $V_{inv}(G_{n-1})$ represents the inverter voltage to obtain the maximum output power at low insolation G_{n-1} while $V_{pv}(G_{n-1})$ is the PV voltage at that insolation. As insolation increases from G_{n-1} to G_n, the PV voltage at which the same output power is required increases to $V_{pv}(G_n)$. Using PV characteristics at different insolations and temperatures combined with the inverter characteristics a relationship can be established between change in insolation ΔG and Δm_a at several temperatures T, as:

$$\Delta m_{a_k} = \frac{V_{inv}(G_{n-1})}{V_{pv}(G_n)} - \frac{V_{inv}(G_{n-1})}{V_{pv}(G_{n-1})} \qquad (4)$$

It should be noted that the permissible working area of the proposed set is located under the intersection between the inverter and PV characteristics as given in figure8.

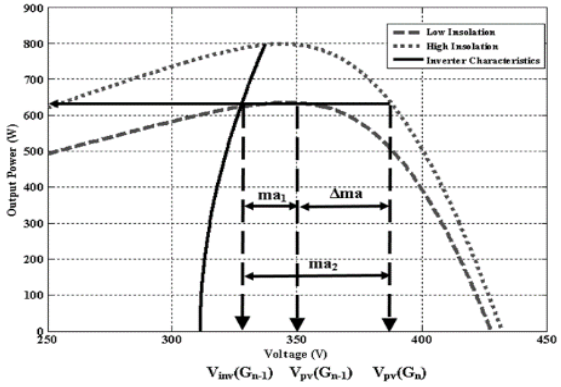

Fig.8 Change in m_a due to change in insolation

SIMULATION RESULTS

The proposed algorithm has been simulated on a system with the specifications given in Table I. The inverter voltage was calculated using Equation (2) for the entire operating range and checked to satisfy the PV output voltage throughout different insolations, and the L-filter has been adopted based on the method introduced by the authors in [7].

Table I: System Parameters

V_q	220
Number of series PV modules	20
PV array total maximum power	800W
L_1	80mH
C_{dc}	10mF
m_{amax}	0.98
Settlement Range	±0.002
Δm_a	0.005
Algorithm Sampling Rate	0.1 sec

A. The Proposed Sensor-less Configuration

In Fig.9, the simulation is presented where the algorithm was executed and tracking process is active from 3 to 22 seconds with noticeable increase in m_a as shown in Fig.10. The algorithm switches to recharging process during 22 to 26 secs due to increase of m_a beyond the limits while DC link capacitor recharges as shown in Fig.10. After m_a settlement the algorithm sets P_{ref} to the previous maximum operating point (*MPP(1)*) and maintains the current operating point as illustrated in Fig.9 at 26 to 40secs during the Observation process. After 40 secs, the insolation is increased to maximum, the algorithm returns back to the tracking process repeating the entire sequence up to the observation process again (*MPP(2)*). After 75 secs, the insolation is decreased to half the maximum. The voltage collapses and m_a increases beyond m_{amax}. The algorithm shifts to zero output power and waits for m_a to settle while the DC link capacitor recharges. The tracking process restarts again in order to achieve (*MPP(1)*). In Fig.11 it is seen that I_g is constant at each *MPP* with no perturbation.

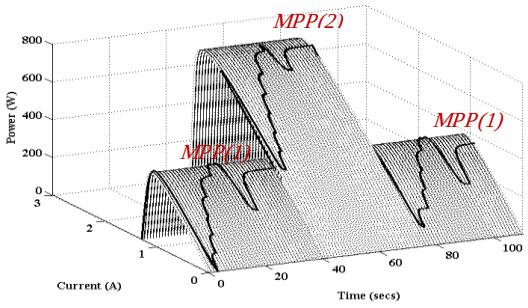

Fig.9. Simulation result for proposed sensor-less *MPPT*

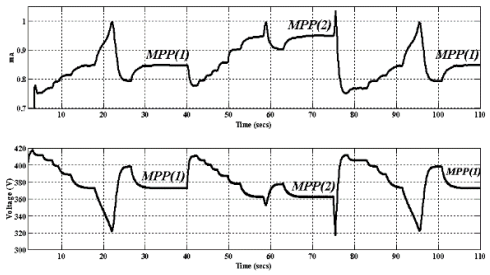

Fig.10. Simulation results of m_a and V_{dc} during the proposed algorithm operation.

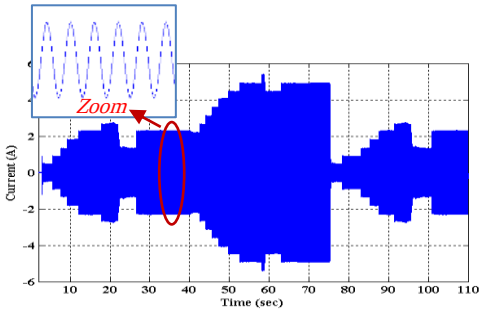

Fig.11. Simulation result for I_g with the proposed *MPPT*

B. Configuration with Sensors

The classical method for *MPPT*, using perturb and observe algorithm with both voltage and current measurements on the DC side, has been also simulated for comparison. The simulation results in Fig.12 show that the response of the configuration with sensors due to insolation changes and *MPPT* is much faster than the proposed technique. This is due to the fact that the sensor-less algorithm requires a low sampling rate in order to detect changes in m_a. Meanwhile, the sensor-less algorithm current oscillations are minimal; since when the system yields maximum power, the algorithm halts until changes occur. Whereas, the sensor-less technique in Fig.13 keeps on perturbing the system to determine changes in the maximum power which yields grid side current oscillations.

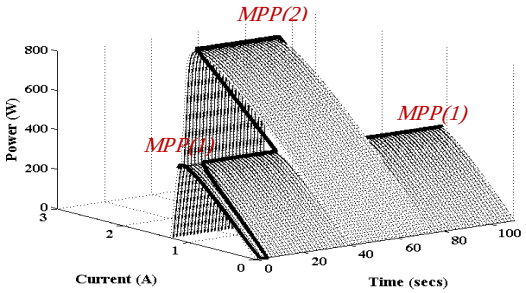

Fig.12. Simulation results of the classical perturb and observe algorithm with sensors during insolation changes

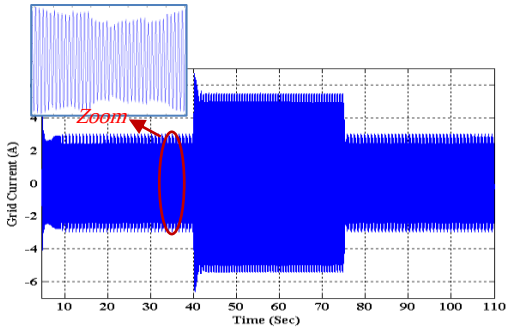

Fig.13. Simulation result for I_g with sensors for MPPT

EXPERIMENTAL RESULTS

The proposed configuration has been implemented based on Table I parameters scaled down by 20. A Texas Instruments TMS320F28335 32-bit microcontroller was used as a controller and a FAIRCHILD Smart Power Module FSBB15CH60C as the inverter. The output grid current waveform shown in Fig.14 was recorded on a digital oscilloscope and then redrawn. Fig.14 consists of 8 operation regions. In Region (2) the algorithm was executed and started the tracking process. In Region (3), the algorithm shifts to recharging process and then to observation process where the algorithm moves directly to the previous output power noted by (MPP(2)). At T=40sec, partial shading was applied to imitate the effect of decrease in solar insolation. Region (4) shows the reduction in the output power up to the maximum output power at (MPP(1))to the observation process in Region(5). At T=55sec, partial shading was removed and the tracking process is continued in Region (6). Region (7) represents operation at the *MPP* during the observation process at MPP(2). Finally in Region (8) the controller was switched off.

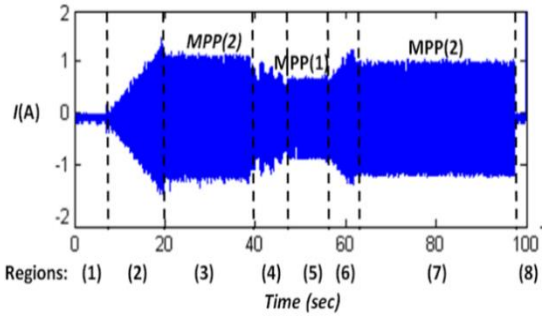

Fig.14. Experimental results of the output grid current using the proposed technique (without any DC bus sensor) during variation of the PV available MPP

CONCLUSION

A new sensor-less PV *MPPT* algorithm was developed and evaluated for a single-stage grid connected inverter. The proposal has been simulated and experimentally tested where the obtained results showed the effectiveness of the set to nearly track the maximum available PV power without using any sensors in DC side. The main limiting disadvantage is the slow response of the system comparing with same set using sensors. This slow response could be accepted for PV tracking application particularly as it also has the advantage of providing lower ripple grid current.

REFERENCES

[1] S.B. Kjaer, J.K. B.F. Pedersen, 2005, "A review of single-phase grid-connected inverters for photovoltaic modules", IEEE Trans. on Ind. App., vol.41, no.5, 1292-1306

[2] N.A. Rahim, J. Selvaraj, 2007,"Hysteresis current control and sensorless MPPT for grid-connected PV systems", IEEE Int. Symposium on Ind. Electronics, 572-575

[3] T. Kitano, M. Matsui, De-hong Xu, 2001" Power sensor-less MPPT control scheme utilizing power balance at DC link-system design to ensure stability and response", IEEE Conf. of Ind. Electronics Society, vol.2. 1309-1314

[4] S. Park, A.K. Jinda, A.M. Gole, M. Park, I. Yu, 2009"An optimized sensorless MPPT method for PV generation system", Canadian Conf. on Elec. and Comp. Eng., 720-724

[5] S. Jain, V. Agarwal, 2007 "Comparison of the performance of maximum power point tracking schemes applied to single-stage grid-connected photovoltaic systems", IET Electric Power Appl., vol.1, no.5, 753-762

[6] H. Patel, V. Agarwal, 2009 "MPPT scheme for a PV-fed single-phase single-stage grid-connected inverter operating in CCM with only one current sensor", IEEE Trans. on Energy Conversion, vol.24, no.1, 256-263

[7] M.A. Elsaharty, H.A. Ashour, 2014, "Passive L and LCL filter design method for grid-connected inverters", ISGT2014, IEEE Innovative Smart Grid Technologies Conf. 13-18